

CAUSAL INFERENCE IN ENERGY DEMAND PREDICTION

CHUTIAN MA, GRIGORII POMAZKIN, GIANCINTO PAOLO (GP) SAGGESE,
AND PAUL SMITH

ABSTRACT. Energy demand prediction is critical for grid operators, industrial energy consumers, and service providers. Energy demand is influenced by multiple factors, including weather conditions (e.g. temperature, humidity, wind speed, solar radiation), and calendar information (e.g. hour of day and month of year), which further affect daily work and life schedules. These factors are causally interdependent, making the problem more complex than simple correlation-based learning techniques satisfactorily allow for. We propose a structural causal model that explains the causal relationship between these variables. A full analysis is performed to validate our causal beliefs, also revealing important insights consistent with prior studies. For example, our causal model reveals that energy demand responds to temperature fluctuations with season-dependent sensitivity. Additionally, we find that energy demand exhibits lower variance in winter due to the decoupling effect between temperature changes and daily activity patterns. We then build a Bayesian model, which takes advantage of the causal insights we learned as prior knowledge. The model is trained and tested on unseen data and yields state-of-the-art performance in the form of a 3.84% MAPE on the test set. The model also demonstrates strong robustness, as the cross-validation across two years of data yields an average MAPE of 3.88%.

CONTENTS

1. Introduction	1
2. Analysis of Causal Structure	2
3. A Full Bayesian Treatment	10
4. Conclusion	16
5. Future Directions	16
Appendix A. Legitimacy of Approach 2	16
Appendix B. Parameters and Priors	17
References	19

1. INTRODUCTION

While machine learning (ML) has achieved enormous success in recent decades, most modern machine learning systems operate purely on statistical correlation, without any understanding of causation. They excel at detecting patterns in training data, but cannot distinguish between relationships that merely happen to occur together and those that represent genuine cause-and-effect mechanisms. As Bernhard pointed out in [15], this distinction represents one of the most profound gaps

between current AI capabilities and human intelligence and it hinders the ability of AI systems to generalize what they have learned to new problems.

Due to these limitations of correlation-based AI, the machine learning community has shown increasing interest in incorporating causal inference in machine learning [7, 17, 6, 3], and particularly for time series prediction [9, 14].

In terms of “hindering the generalization ability”, the presence of confounder bias stands as one of the most common challenges. In this paper, we define a confounder in the same way as in Pearl’s work on causality (e.g., [11]).

Definition 1.1 (Confounder). Suppose the random variables X, Y, Z are causally connected by the following relation $X \leftarrow Z \rightarrow Y$ (Z affects X and Y causally). Then we say that Z confounds X and Y , or that Z is a confounder of the other two variables.

The existence of confounders is often problematic because they create spurious associations between predictors and outcomes. Models learn these non-causal correlations rather than genuine causal effects. This hinders generalization: when the distribution of predictors shifts in deployment environments or under interventions, the spurious patterns learned from confounded training data fail to hold, leading to poor predictive performance in new settings. This is a major limitation of purely statistical approaches operating at the associational level, as Pearl emphasizes in his discussion of the causal hierarchy [12].

In this paper, we study an energy demand prediction problem in which we model the system load using ML approaches. We present a full analysis of the interdependency structure of the various predictors (including weather conditions and calendar information) and energy demand. At the same time, we list common mistakes and consequences originating from confounder bias and misspecified causal structure. A Bayesian causal model is later built based on the causal insights, trained on real-world energy demand data and tested on unseen data. The model is able to produce state-of-the-art predictions, with an average MAPE of 3.88% generated from a K -fold cross validation test. In addition, the model is able to explain the variability found in the data, such as the seasonal-dependent variance (heteroscedasticity) and temperature sensitivity.

This paper is structured as follows. Section 2 presents a full analysis of the interdependency between calendar, weather and energy demand variables. We show that ignoring causal structure can cause a trained model to show confounder bias, severely jeopardizing its generalization to unseen data. Section 3 develops a Bayesian model for causal inference and derives insights into the causal dependencies of energy demand. Sections 4 and 5 summarize our findings and propose future research directions to improve the accuracy of the model. Appendix A provides a formal proof using the backdoor criterion to verify that the model used in Section 3 is causally justified in the sense that no confounder biases are present in the resulting estimates.

2. ANALYSIS OF CAUSAL STRUCTURE

It is well known that calendar variables and weather conditions are among the most useful predictors of electricity consumption. For example, during hot summer days, air conditioning usage drives demand upward, while cold winter days increase heating loads. Similarly, electricity usage follows distinct patterns throughout the

day, regardless of prevailing weather conditions, with commercial loads peaking during business hours and residential consumption rising in the evenings and weekends. Understanding these causal relationships—rather than merely observing their correlations—is essential for building robust prediction models that generalize across seasons, weather conditions, and changing usage patterns. Failure to recognize the underlying causal structure may lead to incorrect attributions of individual variables to the total effect, hindering model generalization in cases where the underlying distributions shift. In this section, we propose a causal structure that explains the interdependency between weather, calendar variables, and energy demand. We show that missing certain variables in feature selection not only causes models to lose the predictive power that these variables provide, but may also prevent models from correctly learning the effects of the variables that were selected.

2.1. Dataset Description. We obtained publicly available electricity load data from September 2023 to August 2025 from the Upper Great Plains East (WAUE) balancing authority, which belongs to the Southwest Power Pool [13]. To isolate model performance from weather forecast uncertainty, we evaluate models using actual observed weather data.

The historical weather we obtained from the Open-Meteo Historical Weather API [10], which provides ERA5 reanalysis data [5] at hourly resolution. The weather variables include temperature (2 meters from the ground), wind speed (10 meters from the ground), relative humidity (2 meters from the ground) and solar radiation. For simplicity, weather from the location $\text{LATITUDE} = 44.6321$, $\text{LONGITUDE} = -100.2753$ is chosen as representative of the whole Upper Great Plains East region.

2.2. Structural Causal Model. Our causal treatment is largely based on Pearl’s causality framework. The causal mechanism between variables is represented as a directed acyclic graph (DAG), where each node represents a variable and a functional relationship is assigned to each edge, which characterizes the influence of a cause on its effect. We consider two major classes of variables: calendar variables and weather variables:

- (1) Calendar variables include hour of day and month of year.
- (2) Weather variables include temperature, humidity, wind speed and solar radiation.

While these variables jointly drive energy demand, their contribution to the total demand can be divided into three major categories, which are non-intersecting: (1) energy consumption due to people’s routine activities; (2) heating, ventilation, and air conditioning (HVAC) needs; and (3) lighting needs:

- (1) Routine activity needs are considered to be the base level of energy consumption during people’s activities, e.g. industrial activities, entertainment, etc. “Base level” means that we do not factor in additional energy costs due to heating or cooling needs in the case of extreme weather or additional lighting needs during evening times.
- (2) HVAC needs represent the additional energy consumption due to heating, ventilation and air conditioning.
- (3) Lighting needs represent the additional energy consumption due to insufficient light (e.g., due to seasonal and hour-of-day effects).

We propose the DAG found in Figure 1 to describe the causal mechanism among these variables. The nodes in rectangular blocks in Figure 1 are the observed vari-

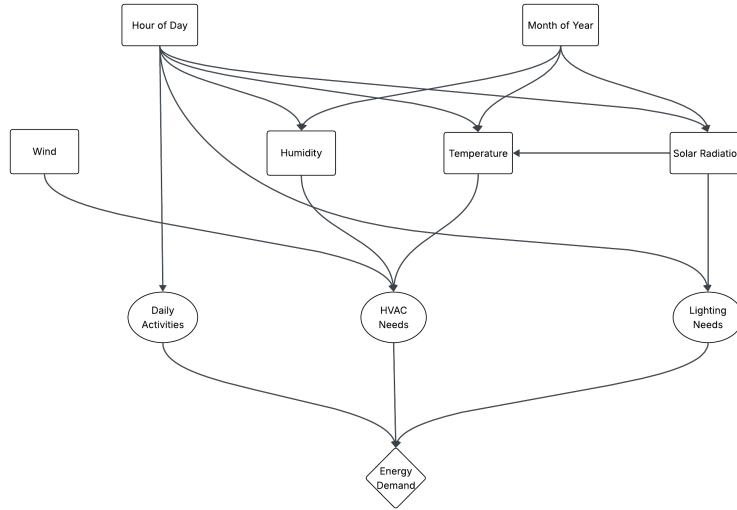


FIGURE 1. Structural Causal Model Driven by Calendar and Weather

ables. The nodes in oval blocks represent three major categories of energy demand. Each arrow represents a cause-and-effect relationship. For example, HVAC needs are jointly determined by temperature, humidity and wind, while these weather variables themselves are affected by the calendar variables hour and month.

2.3. Humidity. In traditional modeling practice, one would only care about the functional relationship between the predictors and the target. Learning relations between predictors is not a typical explicit goal of traditional modeling. However, failing to capture causal effects between predictors, as traditional machine learning techniques fail to do, can lead to erroneous inferences. For example, if one examines the relation between humidity data and energy demand in the WAUE dataset, one will initially notice a negative correlation, as revealed by Figure 2. In fact, we have

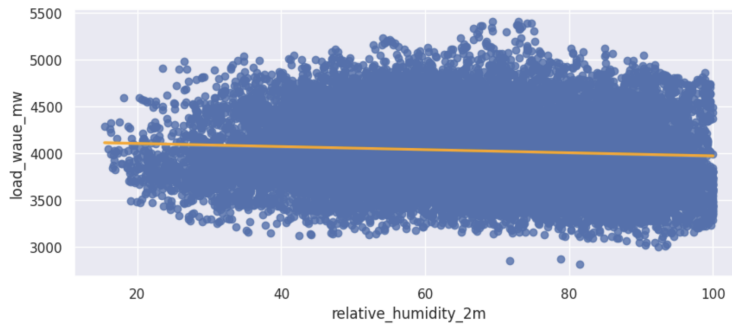


FIGURE 2. Humidity vs. Energy Demand

$$(1) \quad \text{corr}(\text{humidity}, \text{energy}) = -0.07.$$

To quantify uncertainty in the estimated correlation (1), we compute (see Figure 3) the approximate confidence density using Fisher’s z-transform, which provides an excellent approximation to the exact posterior in our regime (see equation (2.11) and discussion in [16]).

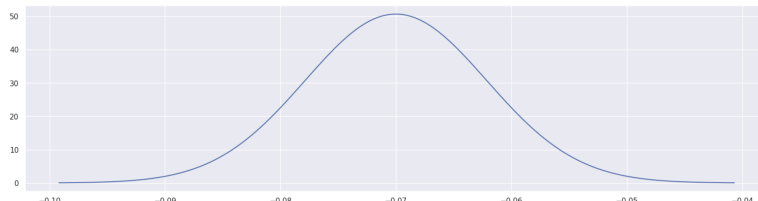


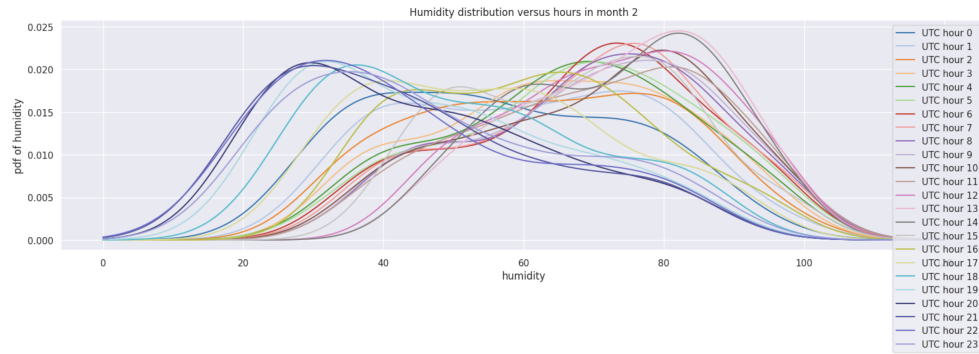
FIGURE 3. The Distribution of Correlation

However, this contradicts domain knowledge, which suggests that higher humidity increases ventilation and cooling needs. This contradiction occurs because we ignored the variable hour of day, which is a confounder of humidity and energy demand, during feature selection. We can verify that humidity is causally affected by hour of the day by examining its conditional distribution, as shown in figure 4. Each curve corresponds to the density function of humidity sampled from a specific hour of the day.

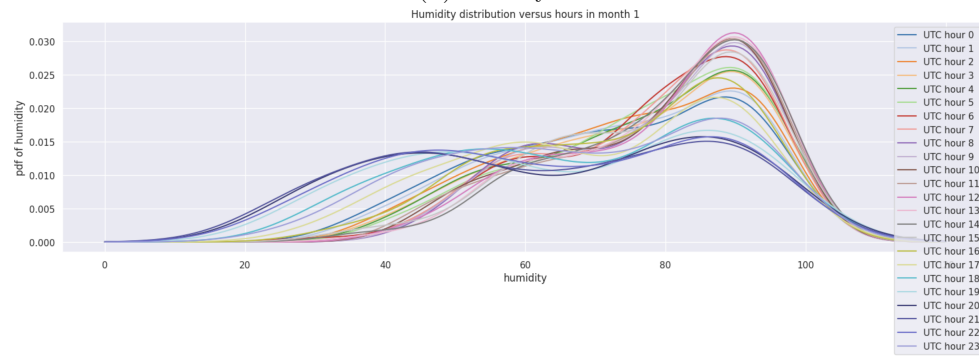
Note that humidity reaches its peak in the morning around 6 a.m. Despite the fact that high humidity tends to increase ventilation and cooling needs, 6 a.m. is an off-peak hour in terms of energy consumption attributable to people’s routine activities. As a result, conditioning on humidity directly increases the HVAC demand, while at the same time has the “unexpected” effect of shifting the time toward an off-peak hour, which indirectly lowers the energy consumption cost. In the end, these two effects sum up to an overall negative correlation as we have seen in Figure 2. The intuition can be visualized in Figure 5 where the black solid path “humidity→HVAC→energy” represents the causal effect of humidity on the energy demand and the red dotted path “humidity←hour→routine activities→energy” represents the implicit effect caused by conditioning on humidity.

In order to address the confounder bias, we need only to control the value of confounders. Figure 6 shows the relationship between humidity and energy demand adjusted for hour and temperature. In the scenario where temperature is high (above a threshold around 75°F), humidity has a positive correlation with energy demand, while this effect diminishes below the threshold. We remark that the standard deviation of the energy demand is 369 MW when we condition the temperature to be above 75°F. Figure 6(A) shows that the effect of humidity can explain a significant portion of the data variability in this scenario, up to 300 MW if we vary the humidity from the lowest to the highest. This observation echoes the importance of incorporating humidity in energy demand forecasting especially in heat events, as pointed out in [8].

2.4. Temperature. Temperature is known as the most important predictor among weather features. In various research efforts (e.g., [1], [4]), it has been pointed out that energy demand is more sensitive to temperature changes during summer and winter than it is to temperature changes during spring and fall. There exists a comfortable temperature zone (typically around 65-70°F) away from which the energy



(A) January



(B) February

FIGURE 4. The Distribution of Humidity Against Month and Hour

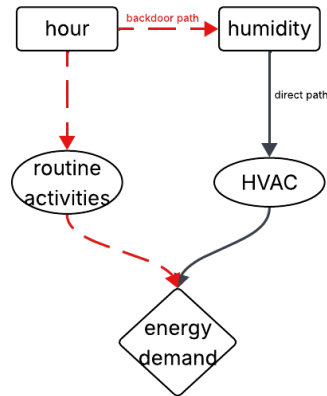
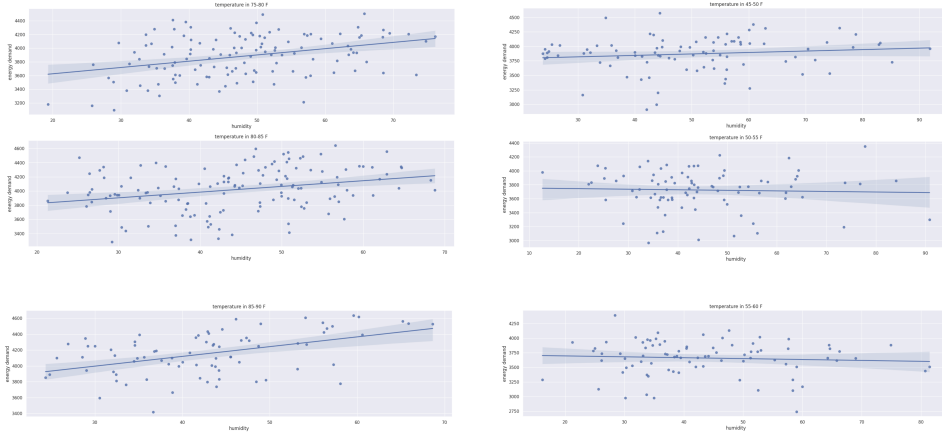


FIGURE 5. Direct Path and Backdoor Path



(A) High Temperature Scenario

(B) Mild Temperature Scenario

FIGURE 6. Humidity vs. Energy Demand: Adjusted for Hour and Month

demand increases drastically. As such, spring and fall with milder temperatures falling inside the comfortable zone are often called “shoulder seasons” in the energy industry. In contrast, during summer and winter, when temperatures deviate substantially from the comfort range, even small temperature changes can trigger large swings in electricity consumption. This behavior is observed in our dataset, as shown in Figure 7.

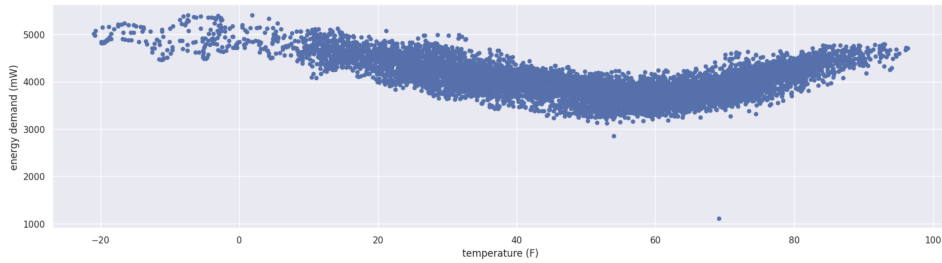


FIGURE 7. Nonlinear Relation Between Temperature and Energy Demand

Motivated by Figure 7, we transform the raw temperature using equation 2,

$$(2) \quad T_{\text{transformed}} = |T - T_{\text{midpoint}}|,$$

where T_{midpoint} refers to the midpoint between hot and cold extremes when both heating and cooling needs are minimized (e.g., in the most temperate season for the geography in question). In this paper, the temperature midpoint T_{midpoint} is chosen to be 56°F, which best fits the observed data. We further make the assumption that the energy demand E depends on temperature via

$$(3) \quad E = \lambda(M)T_{\text{transformed}} + \text{noise}$$

where M , ranging from 1 to 12, refers to months, and $\lambda(\text{month})$ is the month-dependent coefficient of the temperature predictor, reflecting the fact that energy demand responds to temperature changes differently in each season. To learn these monthly coefficients, we fix the month and run linear regression based on (3), using the transformed temperature as the regressor and energy demand as the target.

Note that even after we condition on month, the variable “hour of day” still confounds both temperature and energy demand. We have to adjust for its value to learn the unbiased effect of temperature. This can be accomplished simply by incorporating hour of day and temperature together in a single regression, as illustrated in Approach 2 below. In Appendix A, we show that this simplified approach is equivalent to conditioning on month of year and hour of day and estimating the causal effects in the resulting subgroups. This will be compared with the naive approach as illustrated in Approach 1, where one attempts to align the transformed temperature and energy demand in a regression without adjusting for the hour of day as confounder.

Approach 1 (Non-causal, learn biased estimate). Perform two regressions. The first linear regression uses $T_{\text{transformed}}$ as the regressor and energy demand as the target. A subsequent regression then uses the trigonometric functions of hours as the regressor, which represent the 24-hour daily cycle, and the residuals of the first regression as the target.

Approach 2 (Causal, no bias). Perform a full regression with temperature and daily cycle as regressors and energy demand as target. The daily cycle is represented by harmonics (trigonometric functions) of hours.

We compare the estimates of these approaches by training both models on 2024 monthly data and testing on 2025 monthly data. The results are evaluated by mean average percentage error (MAPE), as presented in Figure 8.

Approach 1, which neglected the causal structure and the existence of confounding, resulted in 47.8% deviation in the estimated coefficients compared to Approach 2, and a 12.5% worse out-of-sample MAPE on average. Intuitively, this bias was created due to the facts that

- (1) Temperature affects cooling and heating needs, which drives the energy demand directly.
- (2) The daily cycle affects the energy demand through two mechanisms:
 - (a) People’s work and life schedules depend upon particular times of day, which affect energy consumption,
 - (b) The hour of day affects the temperature, which further affects the energy demand.

A sample with a high temperature is more likely to be taken in midday, which happens to be a peak hour in terms of energy consumption by people’s daily activities. On the other hand, samples with low temperature are more likely to be taken after midnight, when most people are asleep and do not consume energy due to work/life activities. Without adjusting for hour, Approach 1 incorrectly attributes partial effects of the 24-hour cycle into that of temperature. In summer, the peak of activity-induced demand aligns with the peak of cooling demand in midday. This causes Approach 1 to overestimate the effect of temperature in summer. On the

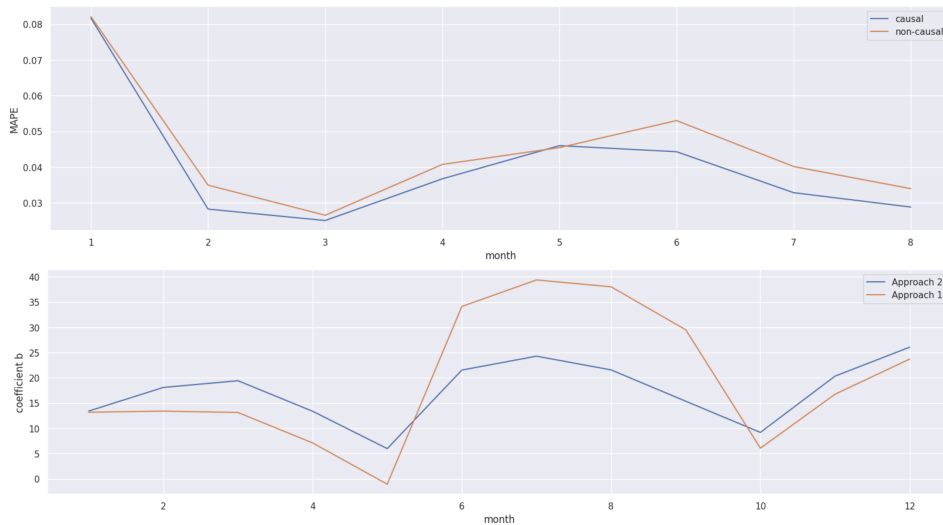


FIGURE 8. Estimates of Approach 1 and Approach 2

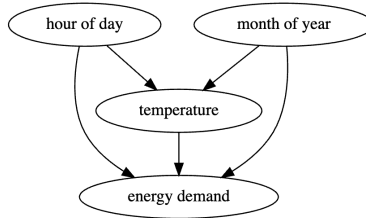


FIGURE 9. Partial DAG Involving Temperature

contrary, winter heating demand peaks after sunset when the activity-induced demand declines. This decoupled effect results in a less volatile energy demand profile in winter with smaller variance.

Remark. If all of the causal relations in a model are linear, then one can avoid the mistake of Approach 1 by invoking the Frisch–Waugh–Lovell theorem, which states that if the regression we are concerned with is expressed in terms of two separate sets of predictor variables:

$$(4) \quad Y = X_1\beta_1 + X_2\beta_2 + u,$$

then β_2 can be learned from a modified regression

$$(5) \quad M_{X_1}Y = M_{X_1}X_2\beta_2 + M_{X_1}u$$

where $M_{X_1}Y$ is the residual of Y after performing a linear regression against X_1 and similarly for $M_{X_1}X_2$. Our experiments have shown that using the Frisch-Waugh-Lovell theorem yields approximately the same results as Approach 2. This can be extended to situations in which the target is a linear combination of predictors after feature engineering. However, in more general situations where the dependency

cannot be transformed into linear relations easily, it is essential to recognize the underlying causal structure to avoid introducing bias into predictions.

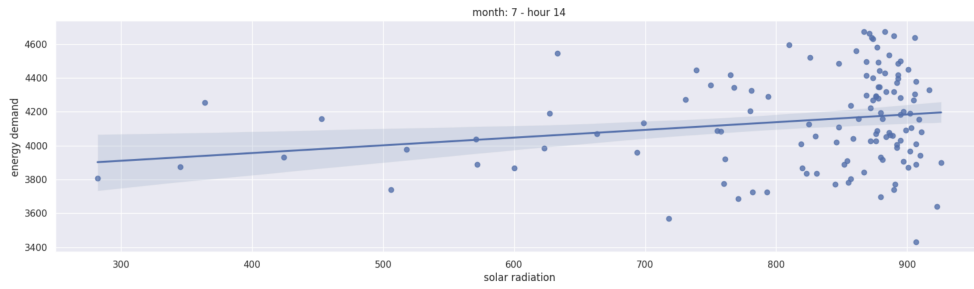
2.5. Solar Radiation. Next, we analyze the effect of solar radiation on energy demand. Intuitively, insufficient natural light boosts the demand for artificial light. Figure 10 shows this effect using samples taken from the month of July and from different hours. It is shown that the energy demand responds to solar radiation differently in different regimes similar to the effect of temperature, in the sense that there exists certain thresholds beyond which further increasing sunlight no longer decreases the energy consumption. In Figure 10a, it even appears as if brighter sunlight increases the energy demand substantially in summer. This, however, can be easily traced down in the causal DAG 1 to the effect of temperature: in the summer, greater solar radiation warms the air and increases the air temperature, which translates to greater cooling demand. As one would expect, during winter, increasing solar radiation leads to warmer air and thus lower heating needs, as shown in Figure 10c.

2.6. Wind Speed. Wind is related to energy demand, as it affects HVAC demand. This effect must be evaluated jointly with temperature. Figure 11 shows that strong winds decrease energy demand in hot weather and increase it in cold weather. A possible explanation is that the wind causes indoor spaces to lose heat faster, which reduce cooling needs in summer and increase heating needs in winter.

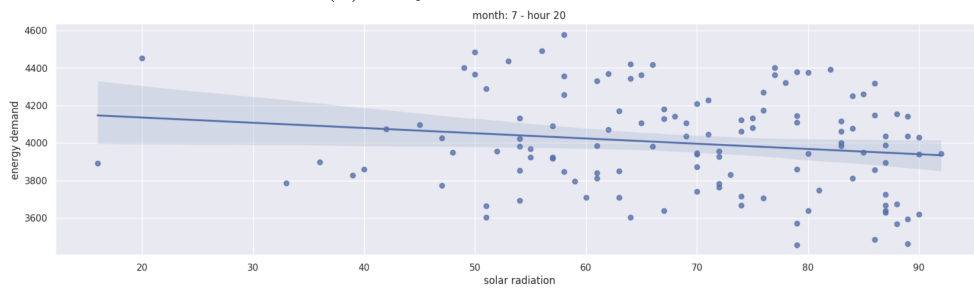
3. A FULL BAYESIAN TREATMENT

3.1. Model Setup. We proceed to transform the causal insights derived in Section 2 into a Bayesian predictive model. Bayesian inference treats model parameters as random variables with probability distributions rather than fixed unknown values. One begins with prior beliefs about parameters, then updates these beliefs using observed data via Bayes’ theorem to obtain posterior distributions that quantify our uncertainty about parameter values. In addition to providing uncertainty estimates, it can take advantage of prior knowledge, e.g. derived from domain knowledge or exploratory studies. In our case, we encode the causal insights from Section 2 into priors and build a Bayesian model on top.

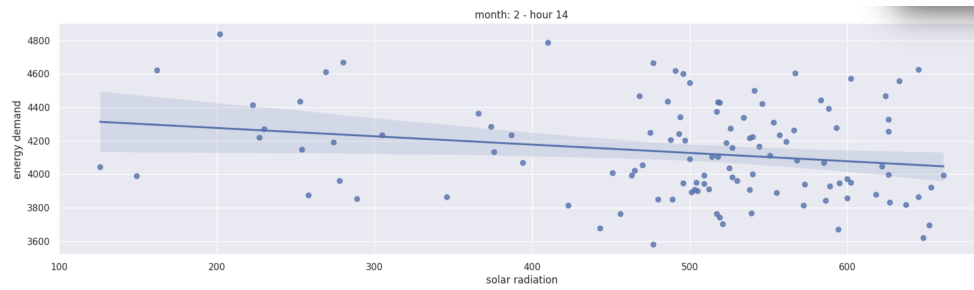
The model is implemented in Python using the Pyro package [2]. It enables us to encode the structural causal model as represented by Figure 1 into a DAG. Each node in the DAG represents an observed variable. The model simulates the data generation process by a set of manually encoded rules. The hour and month are sampled as categorical variables ranging from 0 to 23 and 1 to 12 respectively. These are root nodes, as they do not have parents in the DAG. The sampling of the child nodes depends upon the value of parent nodes. Temperature is sampled from a Gaussian distribution whose mean value is a harmonic series of hour H and



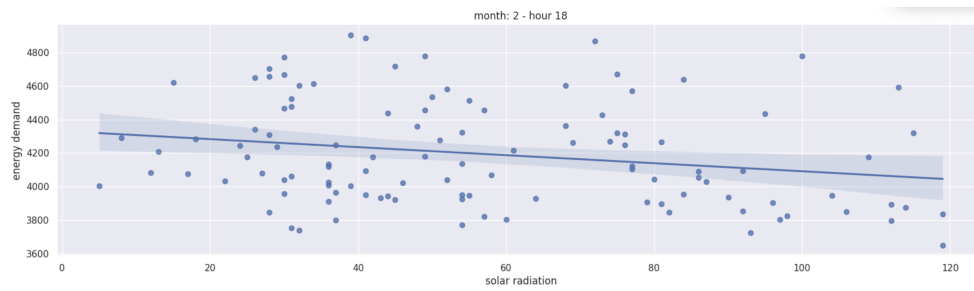
(A) Early Summer Afternoon



(B) Summer Sunset



(C) Early Winter Afternoon



(D) Winter Sunset

FIGURE 10. Solar Radiation vs. Energy Demand

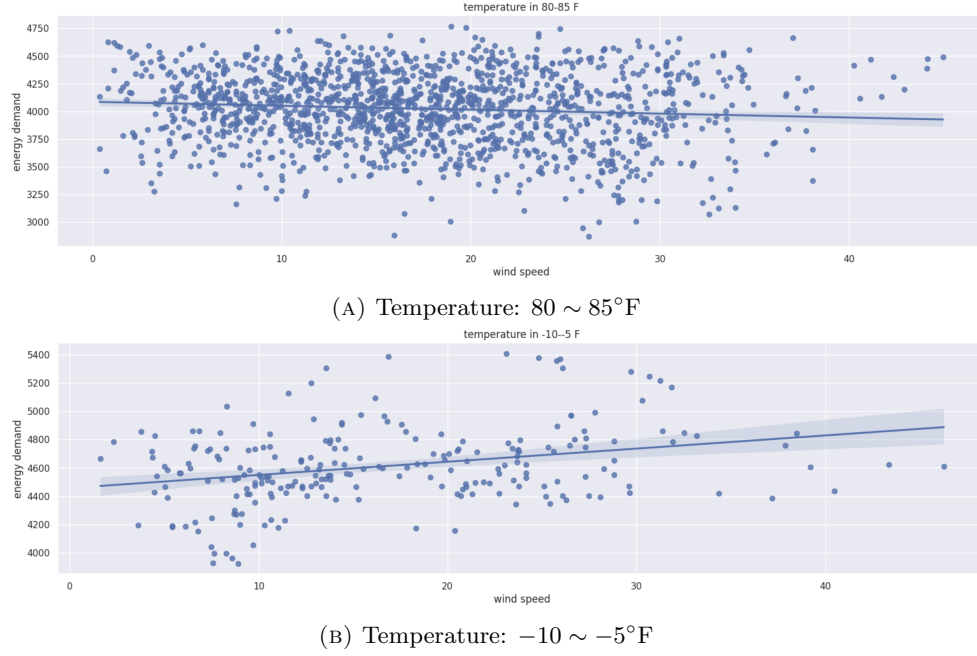


FIGURE 11. Wind Speed vs. Energy Demand

month M :

(6)

$$\begin{aligned}
 \text{Temperature} = & \overbrace{\sum_{j=1}^n (c_j \sin(2\pi j M/12) + c_j^* \cos(2\pi j M/12))}^{\text{yearly seasons}} \\
 & + \underbrace{\sum_{j=1}^n (d_j \sin(2\pi j H/24) + d_j^* \cos(2\pi j H/24))}_{\text{daily temperature cycle}} + w \cdot \text{Rad} + T_{\text{base}} + \underbrace{e_{\text{temp}}}_{\text{noise}},
 \end{aligned}$$

where Rad refers to solar radiation, T_{base} is a constant baseline and $e_{\text{temp}} \sim \mathcal{N}(0, \sigma^2)$ is Gaussian random noise.

We sample humidity from a beta distribution $Beta(\alpha, \beta)$ whose parameters are determined by month and hour.

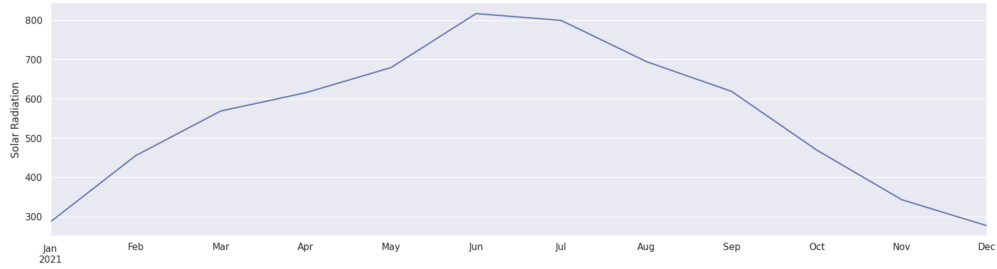
$$\begin{aligned}
 (7) \quad \alpha &= \theta \sin\left(\frac{\pi H}{12}\right) + \theta^* \cos\left(\frac{\pi H}{12}\right) + \alpha_0 \\
 \beta &= \phi \sin\left(\frac{\pi M}{6}\right) + \phi^* \cos\left(\frac{\pi M}{6}\right) + \beta_0 - \alpha
 \end{aligned}$$

The choice of distribution is based on empirical study, which reveals that the concentration and skewness of the humidity distribution are influenced by month and hour, see figure 4, for example, where the shape of the humidity distribution varies greatly by month and hour.

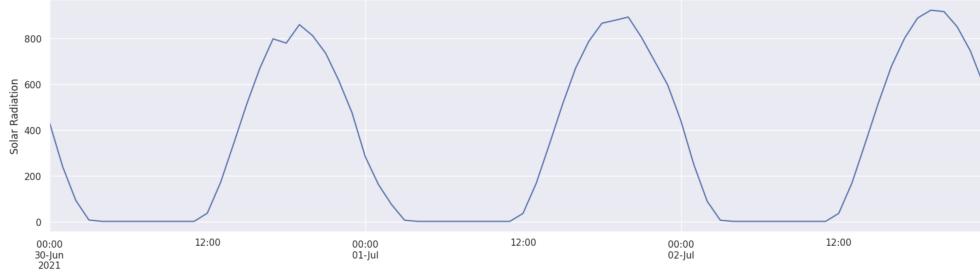
Solar radiation is sampled from a normal distribution and is cast to non-negative values afterwards. The mean of the normal distribution is defined as a function of month and hour, where the effects of month and hour are factorized into separate periodic components.

$$(8) \quad \mu_{\text{Rad}} = \begin{cases} (p \sin(\frac{\pi M}{12}) + q) \sin(\pi \frac{H - H_{\text{sunrise}}(M)}{H_{\text{sunset}}(M) - H_{\text{sunrise}}(M)}), \\ \quad \text{if } H_{\text{sunrise}}(M) \leq H \leq H_{\text{sunset}}(M), \\ 0, \quad \text{otherwise.} \end{cases}$$

where $H_{\text{sunrise}}(M)$ and $H_{\text{sunset}}(M)$ are respectively the local sunrise and sunset time, averaged over the month M . The form of equation (8) is carefully selected based on the empirical results, as shown in figure 12.



(A) Radiation vs. Month



(B) Radiation vs. Hour

FIGURE 12. Solar Radiation vs. Calendar Variables

Wind speed is sampled directly from normal distribution $\mathcal{N}(\mu_{\text{wind}}, \sigma_{\text{wind}})$ and then cast to non-negative values.

Finally, we define the causal effects of these variables on energy demand. The proposed causal DAG 1 states that energy demand can be divided into three disjoint categories: (1) daily activity consumption, (2) HVAC needs and (3) lighting needs. We start with HVAC needs, which is mainly driven by temperature and explains the majority of energy demand variability. Our analysis in Section 2.4 indicates that the relationship between temperature T and energy demand can be approximated by a V-shaped function. In other words, energy demand peaks for both high and low temperatures, and gradually decreases as temperature moves toward some middle

point. Thus, we define the base energy demand to be

$$(9) \quad E_{\text{base}} = kf(T) + E_0$$

where $f(T) = |T - T_{\text{mid}}|$ is the V-shaped function. The term E_0 represents the baseline energy consumption level, which is determined by factors that stay relatively stable, e.g. population, economy, etc.

The humidity affects the HVAC needs on top of the base level. In Section 2.3, we learned that relative humidity $R.H.$ increases energy consumption when the temperature is above some threshold. This effect diminishes when temperature drops back into the comfort-zone. Thus, we model the effect of humidity by

$$(10) \quad E_{\text{humid}} = R.H.\delta(T > T_{R.H.}),$$

where $T_{R.H.}$ is the temperature threshold above which the effect of humidity starts to be visible. In practice, $T_h = 70.0$ is determined via a grid search by maximizing the correlation between Humidity Induced HVAC and energy demand.

Wind (denoted as W) affects energy demand in both high and low temperature scenarios. As pointed out in Section 2.6, strong winds increase energy demand in cold weather and decreases it in hot weathers. We model the effect of wind by

$$(11) \quad E_{\text{wind}} = W\delta(T < T_{w,1}) - \lambda W\delta(T > T_{w,2}).$$

One unit of change in wind speed may cause different amounts of change in energy demand depending upon whether the weather is hot or cold. We introduce the parameter $\lambda > 0$ to model this potential asymmetry. The terms $T_{w,1}$ and $T_{w,2}$ represent the temperature thresholds beyond which the wind's cooling effects become relevant.

Now we turn to the energy consumption due to daily activities. Since daily activities are periodic, we model the demand attributable to them using harmonic series of hours:

$$(12) \quad E_{\text{daily}} = \sum_{j=1}^n (a_j \sin(2\pi jH/24) + a_j^* \cos(2\pi jH/24)).$$

Similarly, the effect of the yearly cycle (e.g. including factors like daylight savings changes) is modeled as a harmonic series of months:

$$(13) \quad E_{\text{yearly}} = \sum_{j=1}^n (\alpha_j \sin(2\pi jM/12) + \alpha_j^* \cos(2\pi jM/12)).$$

The lighting demand is expressed as

$$(14) \quad E_{\text{light}} = \exp(-\beta \cdot \text{Rad})\delta(\text{active hour}).$$

The exponential decay term describes the decreasing need for lighting under sufficient natural light. The $\delta(\text{active hour})$ declares that the lighting demand is only present during active hours, e.g. between 5 a.m. and 12 a.m.

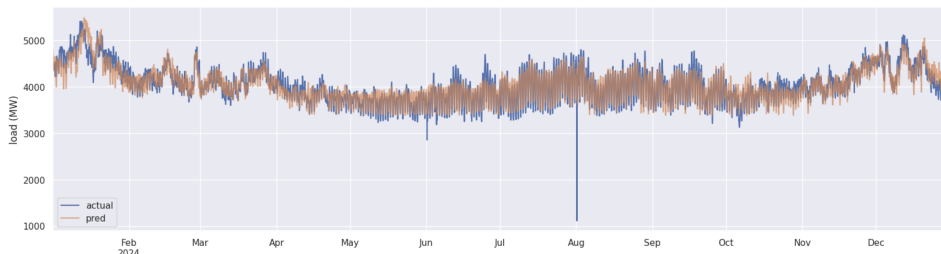
Finally, we sum up all of the individual effects:

$$(15) \quad E = \underbrace{E_{\text{base}} + E_{\text{humid}} + E_{\text{wind}}}_{\text{HVAC needs}} + \underbrace{E_{\text{light}}}_{\text{lighting needs}} + \underbrace{E_{\text{daily}}}_{\text{activity consumption}} + E_{\text{yearly}}$$

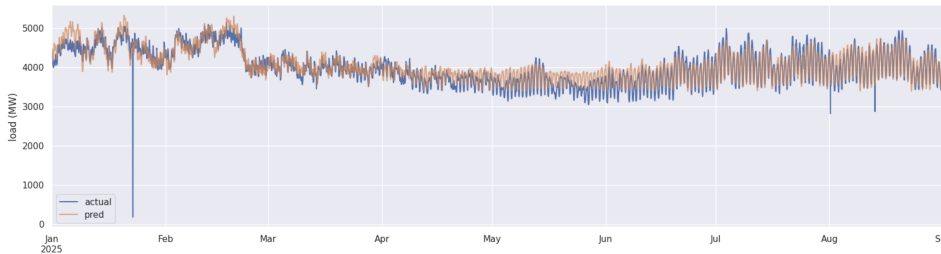
3.2. Training. The specific priors we adopted may be found in Appendix B. After specifying the priors, we condition the Bayesian model on observed data. This step updates our prior beliefs about parameters through the likelihood of the observed data and generates posterior distributions that reflect both our causal assumptions and the observed data.

The posterior distributions are approximated by maximizing the evidence lower bound (ELBO). The ELBO serves as a surrogate objective that balances the likelihood of observing the data given a set of parameters against the complexity of the model. The inference program seeks the set of posterior parameters that maximizes the ELBO. To perform this optimization, we employ stochastic variational inference (SVI), a scalable inference method that uses stochastic gradient descent to approximate the true posterior distribution. An automatic normal guide (AutoNormal) is used to approximate the posterior distributions, which assumes a multivariate Gaussian form with a diagonal covariance structure. The optimization process uses the Adam optimizer with a learning rate of 0.01.

3.3. Performance. The model was trained on data from September 2023 to August 2024 and tested on data from September 2024 to August 2025. Our model achieves a 3.23% MAPE on the training data and 3.84% MAPE on the test set.



(A) In-sample Test



(B) Out-of-sample Test

FIGURE 13. Model Performance

To validate the robustness of our model’s performance, we employed 5-fold cross-validation, partitioning the union of train and test data into five distinct folds where each fold serves as a validation set while the remaining four folds are used for training. This process is repeated five times and the model’s robustness is evaluated by averaging the MAPE across all runs. As a result, the model yields an average MAPE of 3.88%, suggesting consistently strong performance across all folds and no overfitting to specific data characteristics.

Another notable achievement of our model is that it successfully explains the time-varying variance (heteroscedasticity) of the energy demand without requiring explicit variance modeling. We note that electricity demand exhibits significantly larger variance during summer compared to winter. The mechanism underlying this phenomenon is the temporal alignment of causal effects as we pointed out in Section 2: during summer, temperature-induced cooling demand and daily-activity-induced energy consumption both peak around midday, causing these two sources of variation to compound and amplify aggregate demand volatility. In winter, by contrast, heating demand peaks during morning and evening hours when temperatures are lowest, while people’s daily activity remains concentrated during midday. This peaking pattern results in reduced data variance in winter. Compared to pure data driven approaches, our causal approach provides greater explainability and robustness.

4. CONCLUSION

This paper proposed a causal approach for predicting energy demand based on weather features including temperature, relative humidity, solar radiation and wind speed, as well as calendar information including hour of day and month of year. We show that failure to incorporate all the variables that form causal relations with the target can lead to misleading estimates and attributions. In some cases (as we have shown in Section 2.4), not adjusting for the confounder hour-of-day when estimating the effect of temperature on energy demand resulted in a staggering 47.8% bias in the estimated coefficient and a 12.5% loss in MAPE. We also presented a full Bayesian causal model based on the causal structure, which yields robust performance represented by 3.88% average MAPE in a K-fold cross validation test across two years of data.

5. FUTURE DIRECTIONS

We note that the following directions may further improve the model’s performance.

In one direction, more causal features can be incorporated to explain the data variability. For example, week of day was not modeled, but could be of importance for energy demand prediction, since the data pattern is likely to differ based on whether it is a work day or not.

Incorporating temporal dependencies is another potential direction for improvement. Electricity consumption is fundamentally a continuous process with temporal dependencies. When demand exceeds typical levels at time t , it tends to remain elevated at time $t+1$. A natural extension would be to explicitly model this temporal continuity by incorporating autoregressive (AR) components or state space models that capture the evolution of demand over time. However, simply adding lagged demand as a predictor can obscure causal relationships and potentially introduce confounding. Thus, careful consideration of the causal structure is required when integrating historical information into causal models.

APPENDIX A. LEGITIMACY OF APPROACH 2

In this section, we prove that Approach 2 in Section 2.4 is valid for evaluating causal effects under the causal assumptions represented by the causal DAG in Figure 9. Specifically, we show that the regression coefficient between temperature

and energy demand derived from Approach 2 coincides with the causal coefficient defined via the intervention operator in (16).

Definition A.1. Causal effects can be quantified via intervention. For a linear model, the strength of a causal effect can be measured by the coefficient b in

$$(16) \quad \mathbb{E}[y | do(x)] = bx + c.$$

Let the variables x, y, z denote temperature, energy demand, and hour of day, just as in Section 3. Let x^* be the transformed temperature. When performing the linear regression using Approach 2, we essentially assume the following relation: given (condition) the value of x and z , the value of y is a linear combination of x^* and y . No intervention is applied in the process.

$$(17) \quad \mathbb{E}[y | x, z] = a'z + b'x^* + c'.$$

Note that b' learned from conditioning is not the same as the causal coefficient b in general. As we have seen in the case of Approach 1, improper handling of confounding variables will cause bias in our learned results. To this end, the backdoor criterion provides a means to check if we have handled the confounders correctly. In fact, the variable z satisfies the backdoor criterion relative to the ordered pair (x, y) by Definition 3.3.1 in [11]. Thus we have

$$(18) \quad P(y | do(x)) = \sum_z P(y | x, z)P(z).$$

Taking the expectation in z , we have

$$(19) \quad \begin{aligned} \mathbb{E}[y | do(x)] &= \sum_z \mathbb{E}[y | x, z]P(z) \\ &= \sum_z (a'z + b'x^* + c')P(z) \\ &= a'\mathbb{E}[z] + b'x^* + c'. \end{aligned}$$

This shows that the regression coefficient b' coincides with the coefficient b in (16).

APPENDIX B. PARAMETERS AND PRIORS

The priors are specified below.

(1) Parameters for temperature T

$$\begin{aligned} c_1 &\sim \mathcal{N}(-4.6, \sigma_1) \\ c_1^* &\sim \mathcal{N}(6.4, \sigma_1) \\ c_2 &\sim \mathcal{N}(-1.6, \sigma_1) \\ c_2^* &\sim \mathcal{N}(-0.86, \sigma_1) \\ d_1 &\sim \mathcal{N}(-17.0, \sigma_3) \\ d_1^* &\sim \mathcal{N}(-22.0, \sigma_3) \\ d_2 &\sim \mathcal{N}(-2.3, \sigma_3) \\ d_2^* &\sim \mathcal{N}(-2.6, \sigma_3) \\ w &\sim \mathcal{N}(0.01, \sigma_1) \\ T_{\text{base}} &\sim \mathcal{N}(47.0, \sigma_1) \end{aligned}$$

(2) Parameters for humidity:

$$\begin{aligned}\theta &\sim \mathcal{N}(0.5, \sigma_1) \\ \theta^* &\sim \mathcal{N}(-0.7, \sigma_1) \\ \phi &\sim \mathcal{N}(0.3, \sigma_1) \\ \phi^* &\sim \mathcal{N}(-0.3, \sigma_1) \\ \alpha_0 &\sim \mathcal{N}(5.1, \sigma_1) \\ \beta_0 &\sim \mathcal{N}(7.6, \sigma_1)\end{aligned}$$

(3) Parameters for solar radiation:

$$\begin{aligned}p &\sim \mathcal{N}(500.0, \sigma_2) \\ q &\sim \mathcal{N}(300.0, \sigma_2)\end{aligned}$$

(4) Parameters for E_{daily}

$$\begin{aligned}a_1 &\sim \mathcal{N}(-150.0, \sigma_2^2) \\ a_1^* &\sim \mathcal{N}(136.0, \sigma_2^2) \\ a_2 &\sim \mathcal{N}(84.0, \sigma_2^2) \\ a_2^* &\sim \mathcal{N}(7.0, \sigma_2^2)\end{aligned}$$

(5) Parameters for E_{yearly}

$$\begin{aligned}b_1 &\sim \mathcal{N}(-15.0, \sigma_2^2) \\ b_1^* &\sim \mathcal{N}(110.0, \sigma_2^2) \\ b_2 &\sim \mathcal{N}(55.0, \sigma_2^2) \\ b_2^* &\sim \mathcal{N}(45.0, \sigma_2^2)\end{aligned}$$

(6) Parameters for E_{base}

$$\begin{aligned}k &\sim \mathcal{N}(20.0, \sigma_2^2) \\ E_0 &\sim \mathcal{N}(3485.0, \sigma_2^2)\end{aligned}$$

(7) Parameters for E_{humid}

$$\begin{aligned}\mu_{\text{humid}} &\sim \mathcal{N}(63.0, \sigma_2^2) \\ \sigma_{\text{humid}} &\sim \text{LogNormal}(10.0, \sigma_2^2)\end{aligned}$$

(8) Parameters for E_{wind}

$$\mu_{\text{wind}} \sim \mathcal{N}(16.0, \sigma_2^2), \quad \sigma_{\text{wind}} \sim \text{LogNormal}(8.0, \sigma_2^2),$$

(9) Parameters for E_{rad}

$$\begin{aligned}\mu_{\text{rad}} &\sim \mathcal{N}(184.0, \sigma_2^2) \\ \sigma_{\text{rad}} &\sim \text{LogNormal}(167.0, \sigma_2^2)\end{aligned}$$

(10) Noise parameters

$$\begin{aligned}\sigma_1 &= 4.0 \\ \sigma_2 &= 40.0 \\ \sigma_3 &= 10.0\end{aligned}$$

REFERENCES

1. Marie Bessec and Julien Fouquau, *The non-linear link between electricity consumption and temperature in Europe: A threshold panel approach*, *Energy Economics* **30** (2008), no. 5, 2705–2721.
2. Eli Bingham, Jonathan P. Chen, Martin Jankowiak, Fritz Obermeyer, Neeraj Pradhan, Theofanis Karaletsos, Rohit Singh, Paul Szerlip, Paul Horsfall, and Noah D. Goodman, *Pyro: Deep universal probabilistic programming*, *Journal of Machine Learning Research* **20** (2019), no. 28, 1–6.
3. Jennie E Brand, Xiang Zhou, and Yu Xie, *Recent developments in causal inference and machine learning*, *Annual Review of Sociology* **49** (2023), no. 1, 81–110.
4. M Hekkenberg, HC Moll, and AJM Schoot Uiterkamp, *Dynamic temperature dependence patterns in future energy demand models in the context of climate change*, *Energy* **34** (2009), no. 11, 1797–1806.
5. Hans Hersbach, Bill Bell, Paul Berrisford, Shoji Hirahara, András Horányi, Joaquín Muñoz-Sabater, Julien Nicolas, Carole Peubey, Raluca Radu, Dinand Schepers, et al., *The ERA5 global reanalysis*, *Quarterly journal of the royal meteorological society* **146** (2020), no. 730, 1999–2049.
6. Licheng Jiao, Yuhan Wang, Xu Liu, Lingling Li, Fang Liu, Wenping Ma, Yuwei Guo, Puhua Chen, Shuyuan Yang, and Biao Hou, *Causal inference meets deep learning: A comprehensive survey*, *Research* **7** (2024), 0467.
7. Jean Kaddour, Aengus Lynch, Qi Liu, Matt J Kusner, and Ricardo Silva, *Causal machine learning: A survey and open problems*, arXiv preprint arXiv:2206.15475 (2022).
8. Debora Maia-Silva, Rohini Kumar, and Roshanak Nateghi, *The critical role of humidity in modeling summer electricity demand across the United States*, *Nature Communications* **11** (2020), no. 1, 1686.
9. Raha Moraffah, Paras Sheth, Mansooreh Karami, Anchit Bhattacharya, Qianru Wang, Anique Tahir, Adrienne Raglin, and Huan Liu, *Causal inference for time series analysis: Problems, methods and evaluation*, *Knowledge and Information Systems* **63** (2021), no. 12, 3041–3085.
10. Open-Meteo, *Hourly load data*, <https://open-meteo.com/en/docs/historical-weather-api>, 2025.
11. Judea Pearl, *Causality*, 2nd ed., Cambridge University Press, 2009.
12. ———, *Theoretical Impediments to Machine Learning With Seven Sparks from the Causal Revolution*, Proceedings of the Eleventh ACM International Conference on Web Search and Data Mining (New York, NY, USA), WSDM '18, Association for Computing Machinery, 2018, p. 3.
13. South West Power Pool, *Hourly Load Data*, <https://portal.spp.org/pages/hourly-load>, 2025.
14. Jakob Runge, Andreas Gerhardus, Gherardo Varando, Veronika Eyring, and Gustau Camps-Valls, *Causal inference for time series*, *Nature Reviews Earth & Environment* **4** (2023), no. 7, 487–505.
15. Bernhard Schölkopf, *Causality for Machine Learning*, 1 ed., p. 765–804, Association for Computing Machinery, New York, NY, USA, 2022.
16. Gunnar Taraldsen, *The Confidence Density for Correlation*, *Sankhya A* **85** (2023), 600–616.
17. Liuyi Yao, Zhixuan Chu, Sheng Li, Yaliang Li, Jing Gao, and Aidong Zhang, *A survey on causal inference*, *ACM Transactions on Knowledge Discovery from Data (TKDD)* **15** (2021), no. 5, 1–46.

Email address: c.ma@causify.ai

Email address: g.pomazkin@causify.ai

Email address: gp@causify.ai

Email address: paul@causify.ai